RSC Advances

PAPER

View Article Online
View Journal | View Issue

Cite this: *RSC Adv.*, 2021, **11**, 16326

Towards a selective synthetic route for cobalt amino acid complexes and their application in ring opening polymerization of *rac*-lactide†

Andrés Castro Ruiz, Krishna K. Damodaran and Sigridur G. Suman *

Catalysts based on cobalt amino acids and 2,2 bipyridine (bipy) present an attractive and cost-effective alternative as ring opening polymerization catalysts, yet this system remains underexplored despite the advantageous coordination properties of amino acids and bipy as ligands combined with the variety of accessible oxidation states and coordination geometries of cobalt. Here, metal complexes of type [Co(aa)$_2$(bipy)] with amino acids (aa: glycine, leucine and threonine) as ligands are reported. The complexes were characterized spectroscopically (IR, UV-vis and ^{1}H, ^{13}C NMR for diamagnetic species), and by MS spectrometry and elemental analysis. The data reveal that the 2,2 bipyridine acts as a neutral bidentate donor coordinating to the metal ion through two nitrogen atoms and the amino acid acts as a bidentate ligand coordinating through the carboxylate and amino group forming a stable five membered ring and a *pseudo*-octahedral geometry around the Co center. The activity of the complexes for the ring opening polymerization (ROP) of *rac*-lactide is presented. The complexes are effective initiators for the ROP of *rac*-lactide (K_{obs} = 9.05 × 10^{-4} s^{-1}) at 100 : 1 [*rac*-lactide] : [catalyst] 1 M overall concentration of lactide in toluene at 403 K.

Received 14th April 2021
Accepted 19th April 2021

DOI: 10.1039/d1ra02909f

rsc.li/rsc-advances

Introduction

Biodegradable and biocompatible polyesters such as poly(lactic acid) (PLA) are a promising class of oxygenated polymers that have received considerable attention due to their essential properties in diverse applications, ranging from packaging, fibers for bone scaffolds and drug carriers in the controlled release of active compounds.[1–5] PLA is most efficiently synthesized by ring opening polymerization (ROP) of *rac*-lactide (LA) using homogeneous metal complexes as initiators or catalyst.[6] The most active and selective complexes contain metal centers of Al(III),[7] Fe(II)[8] In(III),[9,10] Zn(II)[11–13] and Y(III).[14]

Cobalt based catalysts have been widely used in polymerization reactions and more recently as bio-inspired photocatalysts,[15–22] but they are far less investigated in ROP of cyclic esters. Only a few examples are known of cobalt complexes as catalysts in ROP of LA. These systems include 2-guadinobenzimidazole, amino mono and bis(phenolate), as shown in Fig. 1, and related amino-ethoxide chelating ligands.[23–26] These catalysts have exhibited good activity and well-controlled ROP of LA affording polymers with high molecular weight in absence of rigorously dry solvents and inert atmospheres, making them an interesting system for industrial application. Nonetheless, they underperform in terms of stereoselective control of PLA microstructure, in comparison with other systems, independently of the nature of donor atoms and substituents on the ligands.[27]

Nature uses metalloenzymes as catalysts to convert small molecules selectively with outstanding efficiency. These biological catalysts often feature earth-abundant metals such as Fe, Zn or Co surrounded by protein scaffolds whose incredible performance is attributable to the dynamic coordination environment provided by the first and outer coordination sphere.[28,29] Cobalt is one of the few transition metals identified with significant bio-essential organometallic chemistry, *e.g.* vitamin B$_{12}$ and related coenzymes.[28,30,31] Taking inspiration from nature, increased interest in the synthesis of coordination compounds constructed from biologically based ligands such as amino acid offers advantages such as intrinsic chirality, structural diversity and diverse coordination capabilities making them an attractive class of bio-ligands for the development of new compounds.[32,33] The heterocyclic diamine 2,2′-bipyridine (bipy) and its derivatives provide important functions in coordination and organometallic chemistry due to its strong chelation property and π-accepting effects.[34,35] Moreover, several reports of coordination complexes feature bipy in various applications including biological studies and ROP.[35,36] Early studies reported high reactivity and

Science Institute, University of Iceland, Dunhagi 3, 107 Reykjavik, Iceland. E-mail: sgsuman@hi.is

† Electronic supplementary information (ESI) available: Tables S1–S3 of crystal data summary, S4–S10 of selected bond lengths and angles for **1**, **2**, **1a**, **7**, **9a**, **4a** and **Co(bipy)$_2$Cl$_2$**. Fig. S1–S3 of Molecular structures of **9a**, **4a** and **Co(bipy)$_2$Cl$_2$**. Fig. S4–S30 of NMR spectroscopy, infrared spectra, and HRMS of compounds, and S30–S39 spectroscopy and analysis of polymers. CCDC codes 2060291–2060294 and 2062819–2062821 contain the supplementary crystallographic data for this paper. For ESI and crystallographic data in CIF or other electronic format see DOI: 10.1039/d1ra02909f

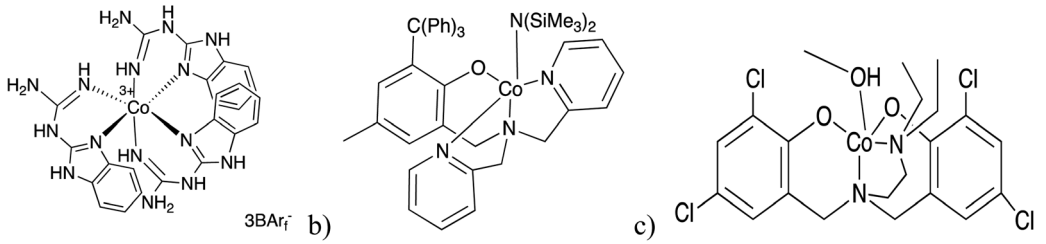

Fig. 1 (a) Cobalt chelate complex of 2-guadinobenzimidazole reported by Gladysz and co-workers.[26] (b and c) Efficient initiators cobalt complexes containing tripodal amino mono and bis(phenolate) ligand.[23,24]

stereocontrolled ROP of lactide mediated by a chiral amino acid as an organocatalyst.[37] Over the last decade research on metal-amino acid compounds has focused on the formation of metal organic framework (MOFs)[38] that exhibit interesting applications in research field such as CO_2 capture,[39] gas separation, and catalysis.[40,41] However, applications of chiral catalysts with single a hexacoordinated metallic center bearing amino acids and bipy as ligands have been limited due to lack of vacant coordination site that is a crucial feature in ring opening polymerization reaction catalysts. Nevertheless this limitation may be circumvented by employing ligands theoretically predicted to be labile in solution.[42–45]

Capitalizing on precedence of successful cobalt based catalysts in ring opening polymerization of *rac*-lactide, a series well-defined mononuclear cobalt complexes containing bipy and commercially available amino acids as ligands were synthesized. In that context, this work describes selective synthesis and detailed characterization of chiral amino acidato bis(2,2-bipyridine)cobalt(II)/(III) complexes. For clarification, separations of geometrical isomer mixtures along with synthesis of analogous amino acid complexes using heterocyclic diamines as ligands the reader is referred to previously reported works in this field.[46–49] As previously stated by Yasui *et al.*, three diastereoisomers are possible for $[Co(aa)_2(bipy)]$ complexes which have achiral amino acidato ligand and possible six diastereoisomers if optically active amino acids are used.[46,47] Hartshorn and co-workers[48] established that a solvent dependence in the equilibria will exist between any secondary reaction products and selective formation of $[Co(aa)_2(bipy)]^+$ when the reaction is performed in aqueous or non-aqueous solvents. Also, results from electrochemical studies of these types of compounds suggest to carry out this reaction under kinetic control in the presence of a strong oxidant such as dioxygen in aqueous solutions if cationic species $[Co(aa)_2(bipy)]^+$ is desired. Based on these observations a synthetic route in an efficient yield towards neutral complexes was designed and different approaches were attempted. In the syntheses, optimization of reaction parameters such as temperature, solvent ratio and order of reagent addition was performed in order to control distribution and formation of thermodynamic or kinetic reaction side-products. This work hypothesizes that an electron rich cobalt center favors coordination-insertion mechanism and that the sigma donor atoms of the amino acids may provide an electronic environment around the metallic center increasing the cobalt center Lewis acidity.[50] Furthermore, the side chains such as hydroxyl/alkyl in the outer coordination sphere may have synergistic effects on the catalytic performance and activity of these compounds.[42,51] With this in mind, to the best of our knowledge, this is the first intentional application of octahedral stereogenic *cobalt amino acid* complexes employed as a chiral catalyst in ring opening polymerization of *rac*-lactide.

Results and discussion

Optimization of parameters and synthesis

The synthetic strategies employed are illustrated in the Scheme 1. The major interest in the synthesized cationic species is their use as a spectroscopic benchmark for the subsequent preparation and characterization of neutral Co(II) analogous complexes.

Cobalt amino acid complexes were synthesized using a one-pot synthesis that consisted of 1 : 2 ratios of bipy, and amino acid and with a subsequent addition of 1 equivalent of CoX_2 (X = Cl^-, OAc^-, NO_3^-) in aqueous ethanol. The complexes isolated were trinuclear Co(II) complexes with the formula $[Co(H_2O)_2(X)_2\{trans(N)\text{-}[Co(aa)_2(bipy)]\}_2]Y_2$ (X = H_2O, Y = Cl; **1**, X = OAc; **4–6**) (bipy: 2,2′ bipyridine; aa: glycine, leucine or threonine), cationic species *trans*(N)-$[Co(aa)_2(bipy)]X$ (X = Cl; **1a–3**, X = PF_6^-; **4a**, X = NO_3^-; **7**) and the neutral species **8–10**.

Synthesis of **1** at room temperature followed by slow addition of $CoCl_2$ led to formation of a mixture of products, which were *cis*-$[Co(bipy)_2Cl_2]$[52] as the major product, and glycinato complex with *trans*-(N) geometry as a secondary product, as well as uncomplexed amino acid and bipy in minor quantities. The products were confirmed using ^{1}H NMR or HRMS-ESI analysis. This observation is in good agreement with stability constants of Co(II) complexes in aqueous solution with bipy ($\log \beta_3 = 17.6$) and glycine ($\log \beta_3 = 10.8$).[44,53,54] In view of theoretical and experimental evidence it is reasonable to expect that the equilibrium kinetically favors the formation of *cis*-$[Co(bipy)_2Cl_2]$.[48] Therefore, it was of interest to evaluate the influence of temperature on the formation of *trans*-(N) isomer.[55] Assuming the reaction rate for the coordination of bipy to Co(II) is faster than the *in situ* deprotonation and subsequent *N*,*O* chelation of glycine; increasing the temperature and employing rapid addition of $CoCl_2$ may reduce the formation of *cis*-$[Co(bipy)_2Cl_2]$. Indeed, this approach was found to readily form two of the desired neutral glycinato complexes with *trans*-(N) geometry isomer units linked *via* tetra-aqua cobalt bridge, with two chloride counter anions. Hence, the formula of **1** can be expressed as $[Co(H_2O)_4\{trans(N)\text{-}[Co(gly)_2(bipy)]\}_2]Cl_2$ that was confirmed by structural analysis using X-ray crystallography. Similar reaction followed by air oxidation led to

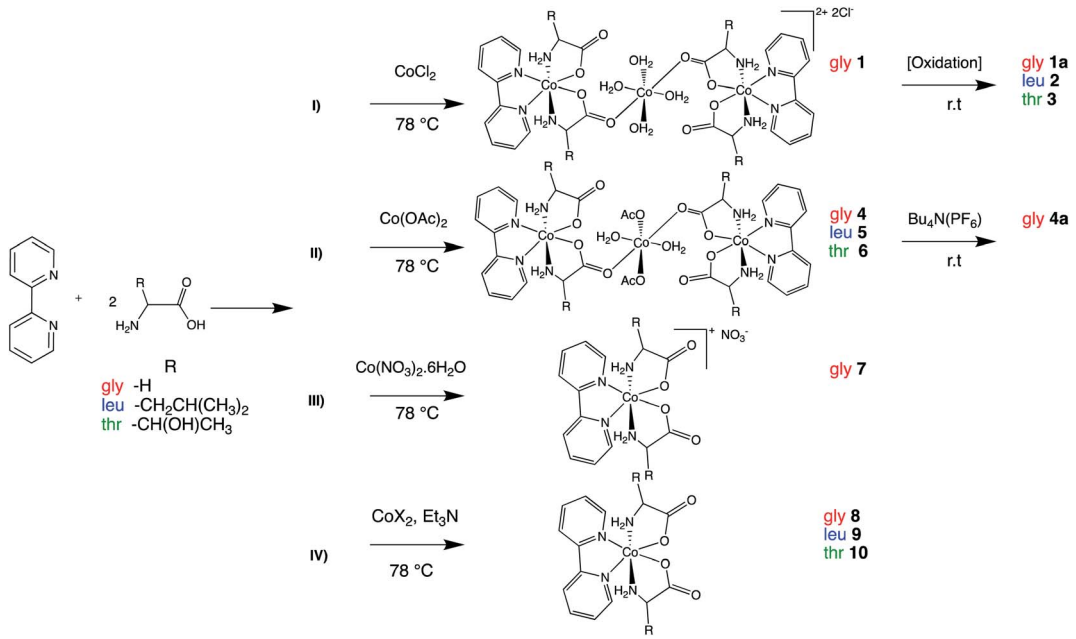

Scheme 1 Synthetic routes (I–IV) for [Co(aa)$_2$(bipy)] **1–10**.

isolation of **1a**, **2** and **3** (Scheme 1(I)) that were also spectroscopically characterized.

As part of the synthesis optimization process, employing cobalt acetate also resulted in successful synthesis of trimetallic complexes **4–6** (Scheme 1(II)). The compound compositions were confirmed by microanalysis of the pink solids obtained. Aerobic reaction conditions during an ion exchange reaction of **4** with (Bu_4N)(PF_6) or a complexation reaction using a cobalt salt with non-coordinating counter-anion such as NO_3^- resulted in cationic species **4a** and **7** (Scheme 1(II) and (III)), respectively.

These experiments resulted in highly reproducible route in good yields to form tri-metallic species. The complexes are air-sensitive and minor air exposure is sufficient to complete oxidation of Co(II) to Co(III).

From a practical perspective, an analogous procedure using CoX_2 (X = Cl, OAc) and triethylamine was carried out in order to evaluate the reactivity of cobalt with other amino acids and bypass the formation of both tri-metallic and ionic compounds. The neutral complexes (**8–10**, Scheme 1(IV)) were isolated as pale pink powders in reasonable >60% yield and were characterized by FT-IR and with high resolution mass spectrometry (HRMS-ESI). The results from this approach indicate that temperature control and the base employed are two major factors that influence whether the *trans*-(N) isomer or any other intermediate species is formed. The neutral complexes are stable as solids under ambient conditions but react slowly with oxygen in the air. In solution **8–10** appear stable for about 24 hours, and after this time an oxidation is observed through a color change of their solutions from pinkish-orange to brownish-red.

Characterization of solid complexes

Structural characterization. Co(II) complex **1** and Co(III) complexes **1a**, **2**, **7**, **4a** were crystallized and structurally characterized. Efforts to crystallize neutral compounds **8–10** under inert atmosphere were unsuccessful; however, slow diffusion of pentane into crude solution of complex **9** in dichloromethane led to isolation of single crystal of cationic complex **9a** with chloride as counter-anion presumed to be derived as contaminant from the reaction

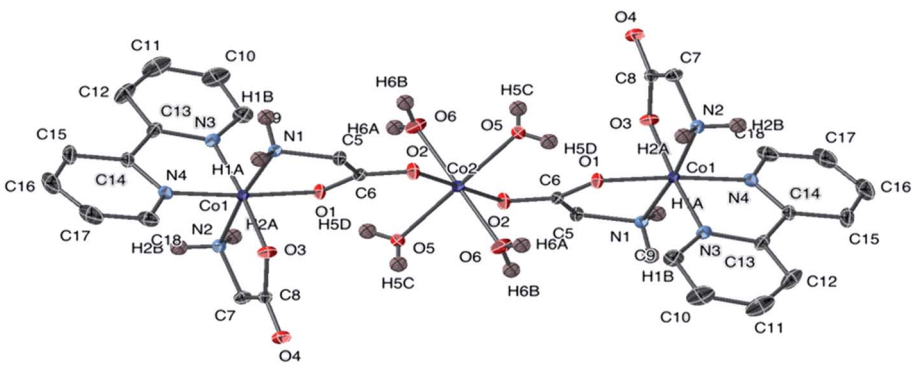

Fig. 2 The structure of the cation of **1** with ellipsoids at 50% probability. Non-amine bound hydrogen atoms are omitted. The counter anion is Cl^- (not shown).

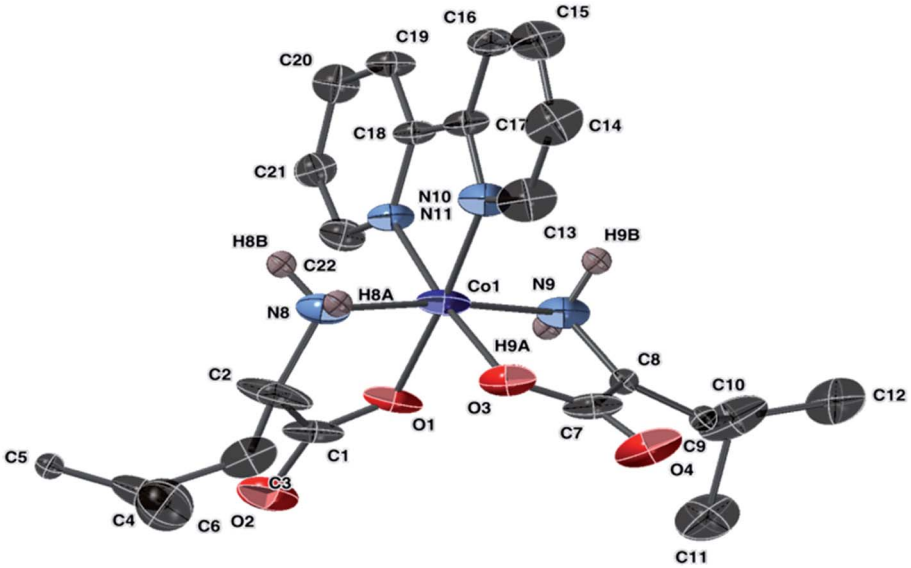

Fig. 3 Molecular structure of the cation of **2**, $[Co(leu)_2(bipy)]Cl$, with ellipsoids at 50% probability. Non amine bound hydrogen atoms are omitted. The counter anion is Cl^- (not shown).

solution. Crystal data is given in the ESI Tables S1–S3,† and selected bond lengths and angles in Tables S4–S10† for **1**, **2**, **1a**, **7**, **4a** and **9a**.

An ellipsoidal plot of **1** at 50% probability is shown in Fig. 2. The structures of **2** and **9a** share same cation; however, the two structures were obtained from different synthetic routes and resulted in crystallization of a chiral molecule **2** and achiral molecule **9a**. The ellipsoidal plot of **2** is given in Fig. 3. Complex **9a** crystallized in a triclinic crystal system, compared to a monoclinic crystal system for direct crystallization of **2**. The structure of **9a** has a disorder that appears solvent dependent and was not completely refined. Fig. S1† depicts the connectivity of the molecule with two crystallographically independent molecules in the asymmetric unit.

Complexes **1a**, **4a**, and **7** share a common cation. Fig. 4 and 5 depict ellipsoidal plots of **1a** and **7**. Figure depicting the ellipsoidal plot of **4a** was placed in the ESI Fig. S2.†

A side product, $Co(bipy)_2Cl_2$ was also crystallized (ESI Fig. S3†) and the structural analysis revealed the formation of

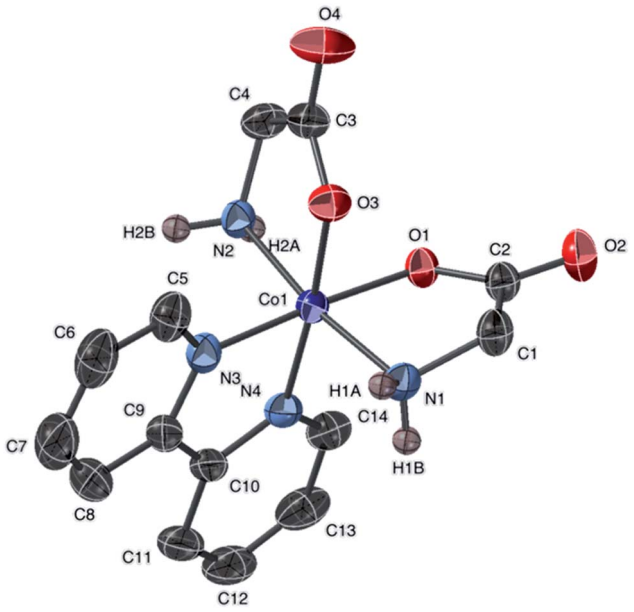

Fig. 4 Molecular structure of the cation of **1a**, $[Co(gly)_2(bipy)]Cl$, with ellipsoids at 50% probability. Non amine-bound hydrogen atoms are omitted. The counter anion is Cl^- (not shown).

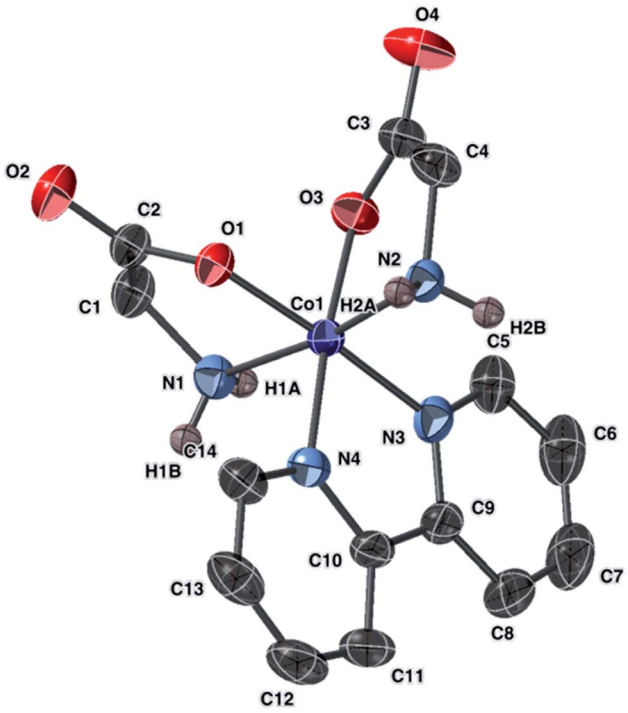

Fig. 5 Molecular structure of the anion of **7** with ellipsoids at 50% probability. Non amine-bound hydrogen atoms are omitted. The counter anion is NO_3^- (not shown).

$Co(bipy)_2Cl_2$, which was crystallized in monoclinic $P2_1/c$. The structure of $Co(bipy)_2Cl_2$ in the solvated form $[Co(bipy)_2Cl_2]\cdot 3H_2O$ has been reported.[52] Therefore, details regarding the crystal data and selected bond lengths and angle are given in Tables S3 and S10.†

Complex **1** was crystallized from aqueous acetone. The X-ray analysis of **1** revealed a trinuclear structure. Two $[Co(gly)_2(bipy)]$ complexes are bridged by tetraaquacobaltate(II) chloride $[Co(H_2O)_4]Cl_2$ molecule co-crystallized in the lattice, as shown in Fig. 2. The Co(II) center adopts hexacoordinated $\{CoO_6\}$ in octahedral geometry between two oxygen atoms of the carbonyl of glycine and the other four positions occupied by oxygen atoms belonging to the four water molecules. The structure shows two hexacoordinated Co(II) center on each side adopting slightly distorted octahedral geometry. Each Co(II) center is coordinated by two nitrogen atoms and two oxygen atoms from the α-amino acid and two nitrogen atoms from 2,2-bipyridine respectively, forming a monomeric unit with three five-membered chelate rings. Selected bond lengths and bond angles values obtained for this complex were found to be in a good agreement with previously reported cobalt complexes of the same category.[56–58]

Complex **2** crystallized in a monoclinic space group $C2/c$. The Co(III) center has a distorted octahedral geometry with the leucine ligands arranged in a *trans-N*,*N-cis*-O,O coordination. The leucine ligands exhibited disorder that was addressed during refinement. Crystals of **9a** revealed a Co(III) center and an overall formula identical to **2**. The data obtained for **9a** appears accurate but contains disordered leucine molecules. The structure was solved but the *R*-factor was high even after the removal of the disordered dichloromethane molecule. Therefore, the data for **9a** is presented in the ESI.† Bond lengths and angles in the molecular unit appear similar for **9a** and for **2**. Co–N bond lengths in **2** and **9a** fall within the range of 1.959 Å to 1.919 Å, and Co–O bond lengths in the range of 1.869 Å to 1.898 Å.

Complexes **1a** and **7** exhibit comparable bond lengths and angles around the Co(III) center. They crystallized in different space groups presumably resulting from the different hydrogen-bond-acceptor strengths of counter anions employed. The glycine bite angles (NH_2–Co–O) fall within the range of 84.77° to 86.40° for all four glycine ligands in **1a** and **7**. Coordination geometry in both crystals is *trans*-N,N–*cis*-O,O with the oxygen atoms of the glycine *trans* to the bipyridine nitrogen donor atoms. Crystals of **4a** (Fig. S3†) have parameters in good agreement with that found for **1a** and **7**.

X-ray analysis revealed that **7** with the formula $[Co(bipy)(gly)_2](NO_3)$ crystallized in an orthorhombic $P2_12_12_1$ space group. The Co(III) metal center displayed a distorted octahedral geometry and the two glycinato anions and the bipyridine moieties were coordinated to the metal center in a chelate fashion. The axial positions were occupied by the nitrogen atoms of the glycinato ion, and the equatorial positions were occupied by the oxygen atoms of two glycinato and the nitrogen atoms of the bipyridine. The non-coordinated nitrate anion interacted with the amino groups *via* non-bonding interaction.

Infrared spectroscopy

Selected FT-IR data of complexes **8–10** are given in the Experimental section and in Fig. S22 –S24.† The three complexes showed broad and strong bands located at high frequencies of *ca.* 3400–3442 cm^{-1} that may be assigned to the OH stretches of water co-crystallized in the lattice. Complexes **8–10** revealed expected IR bands that are similar with significant differences related to the bands expressing differences in the amino acid side chain; an alkyl group at 2870–2957 cm^{-1} for **9** and hydroxyl group at 3390 cm^{-1} for **10**. The bands observed in the range of 3280 cm^{-1} and 2870 cm^{-1} are designated to NH_2 and CH stretching vibrations of amino acids, respectively. These values are slightly shifted to higher energy compared to free α-amino acids (3200–2500), confirming the N-chelation of the α-amino acids to cobalt. Two intense bands with broad profile and a maximum centered between 1640–1660 cm^{-1} and at 1451–1330 cm^{-1} correspond to the asymmetric $\nu_{asym}(COO^-)$ and symmetric $\nu_{sym}(COO^-)$ vibrations modes of carboxylate group, respectively.[59,60] Thus, the difference between these vibration modes *ca* (~290 cm^{-1}) is indicative of monodentate coordination of the carboxylate. Moreover, the complete deprotonation of carboxylic acid was confirmed by the absence of a band normally observed at 1750 cm^{-1}.[61]

As far as bipy ligand is concerned, the vibrations which were attributed to the aromatic stretching vibrations ν(C=C) and ν(C=N) were observed for complexes **8–10** at 1472–1500 cm^{-1}, respectively. Medium absorption peak at ~770 cm^{-1} was assigned to out-of-plane ν(C–H) modes of the ring, shifted to higher frequencies as compared with the free bipy. The IR spectra are consistent with the bidentate coordination of the bipy ligand and N,O-chelation of the amino acids to the metal center.

Characterization of complexes in solution

NMR spectroscopy. NMR 1D (^{1}H and ^{13}C) and 2D experiments (COSY and HSQC) of diamagnetic species were performed. All the assignments were made based on the correlation of NMR spectroscopy data and comparative analysis with similar compounds enabling unambiguous characterization in solution of these complexes. As expected from previous reports coordination of optically active amino acids such as leucine and threonine in bidentate fashion should give rise to a mixture of diastereomers with the metal forming a new stereocenter. To reduce the diastereomeric outcome only enantiomerically pure L-amino acids were used. The complexes **1a**, **4a** and **7** share the same molecular cation containing different counter-anion have similar NMR spectral patterns and will be discussed together.[62] The ^{1}H NMR spectra display resonances with single AB coupling pattern between 3.49 and 3.77 ppm assigned to the methylene protons of the chelated glycinate (Fig. S4†). This pattern is expected for *trans*-(N) isomer due to $-CH_2$ group localized in a chemically equivalent environment in a structure with C_2 symmetry. This configuration was corroborated in the structural analysis of complexes **1a**, **4a** and **7**. ^{1}H NMR in DMSO-d_6 (Fig. S5†) clearly showed upfield shifted amino protons at 5.41 and 6.09 ppm as a consequence of

coordination of the primary amino group. Resonances from 7.89 to 8.72 ppm corresponding to the bipy protons indicate symmetrical mononuclear complex. The ^{1}H and ^{13}C NMR spectral data are consistent with published data for analogous cationic complex involving chloride and perchlorate anions.[46–48] The analysis of 1D and 2D NMR spectroscopy of complex **2** (Fig. S9–S12†) indicated that a mixture of two diastereomers was present in solution assigned as Δ-*RR*/Λ-*SS* and Δ-*SS*/Λ-*RR*. These configurations results in unsymmetrical structures with relative positions of alkyl groups and α-protons on the leucine located in a shielded environment out of the plane of the aromatic rings and it is exactly what is observed in ^{1}H NMR and ^{13}C spectra (Fig. S9 and S11†) that shows chemical shifts with inequivalent intensities for both proton and carbon signals. This observation was corroborated by X-ray diffraction analysis of complex **2** and **9a** which are the same structure with different spatial configuration of the stereocenters. Although the solid structure of complex **3** was not obtained, the NMR spectroscopy (Fig. S13–S17†) of the product clearly shows all the expected resonances for bipy and threonine ligands coordinated to cobalt.

Conductivity, magnetic moment, and mass spectrometry

Neutral complexes **8–10** are highly soluble in polar solvents, hot toluene and slightly soluble in CH_2Cl_2. The molar conductance values of **8–10** at 298 K of 10^{-3} M in ethanol solution are between 11–15 Ω^{-1} cm^2 mol^{-1}, indicating non-electrolytic nature of the complexes. The magnetic moment of **8–10** was obtained using Evans' NMR method,[63] giving an overall effective magnetic moment of 4.24, 4.70 and 4.40 B.M, respectively, which is consistent with three unpaired electrons for $3d^7$ Co(II) and high-spin electronic configuration.[64] These values are slightly higher than the spin-only value reported for a high spin cobalt(II) centre ($\mu_{SO} = 3.87\ \mu_B$, for $S = 3/2$), suggesting significant spin orbit coupling. Such orbital interactions are typically observed in high-spin Co(II) centers for N_4O_2 donor atoms sets,[65] owing to the degeneracy of the triplet ground state, $^{4}T_{1g}$.[66] The complexes were further analyzed by high resolution ESI-MS in positive mode using MeOH as solvent (Fig. S27–S29†). Molecular cation peaks at $m/z = 363.05$, 475.18 and 451.10 were obtained for **8**, **9**, and **10**, respectively, confirming the complexes composition.

Electronic absorption spectra

Electronic spectral data for complexes **8–10** are listed in the Table 1. All spectra are quite similar in the UV region where strong ligand-based absorptions predominate. Fig. 6 shows two bands for complexes **8–10** in the 315–230 nm region. All the bands observed in this region exhibit bathochromic shifts compared to the free ligands. The high intensities bands arise from n–π* and (π–π*, LMCT) charge transfer transitions from donating groups of the ligands to the metallic center. Co(II) bands are *Laporte* forbidden transitions to doublet states and are assumed to be too weak to be visible. The d–d transition bands are rather weak compared to the pronounced n–π* and π–π* absorption bands, thus quantification of d–d transitions for complexes **8–10** was recorded separately at higher compound concentrations in EtOH (5×10^{-3} M). A low-energy absorption band centered at 480–500 nm is attributed to the transition ($^{4}T_{1g}(F)$ $^{4}T_{1g}(P)$) of the high-spin cobalt(II) ions in octahedral geometry.[67]

Table 1 Molar conductance, absorption maxima, molar extinction coefficients and magnetic moment for **8–10**

Compounds	Λ_M[a] (Ω^{-1} cm^2 mol^{-1})	λ_{max} (nm)	(ε (L cm^{-1} mol^{-1}))	μ_{eff} (B.M)
8	12.9	299	(7115)	4.24
		309	(6698)	
		501	(36)[b]	
9	13.1	299	(7740)	4.70
		308	(7104)	
		487	(47)[b]	
10	13.9	301	(7717)	4.40
		309	(7648)	
		488	(35)[b]	

[a] Molar conductance values at 298 K of 10^{-3} M ethanol solution Ω^{-1} cm^2 mol^{-1}. [b] Recorded in 10^{-3} M ethanol solutions.

Ring opening polymerization (ROP)

Complexes **8–10** were evaluated as catalysts in the ROP of *rac*-lactide (LA). Representative polymerization data are summarized in Table 2. The experiments were conducted using a standard set of conditions which were typically at 403 K in toluene solution ([cat] : [LA] 100 : 1). When required, benzyl alcohol (BnOH) was added as a co-initiator (1 equivalent, 3.5 μL). Comparison between **8–10** and other cobalt-catalyst system is difficult since different authors report catalyst performance under dissimilar range of conditions.[24,26] All three complexes displayed high catalytic activity towards ROP of *rac*-lactide either in the presence of an exogenous alcohol or without.

In all cases, polymer kinetics showed a *pseudo* first-order dependence on *rac*-lactide concentration on polymerization

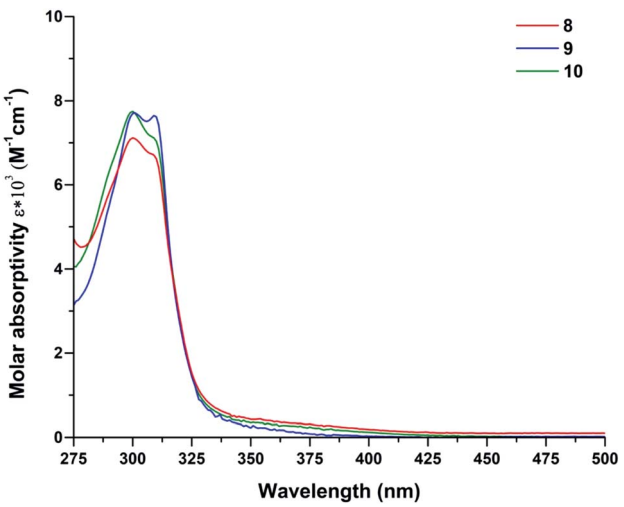

Fig. 6 UV-vis absorption spectra of **8–10** in EtOH (5×10^{-5} M).

Table 2 ROP of *rac*-lactide initiated by **8–10**[a]

Entry	Catalyst	Time (min)	$M_{n,theo}$[c] (kg mol^{-1})	$M_{n,obs}$[d] (kg mol^{-1})	P_i[e]	$Đ$[f]	Conv.[g] (%)
1	**8**	60	13.54	12.39	0.65	1.11	94
2	**9**	60	10.52	15.33	0.54	1.13	73
3	**10**	60	13.11	19.52	0.49	1.22	91
4	**8**	100	14.27	15.36	0.60	1.13	99
5	**9**	100	13.84	34.60	0.59	1.28	96
6	**10**	100	13.98	21.97	0.50	1.40	97
7[b]	**8**	240	12.35	0.14	—	2.02	85
8[b]	**9**	180	3.86	0.32	—	2.04	26
9	**1a–3**	240	—	—	—	—	Traces

[a] Reaction conditions: [LA] : [catalyst] = 100 : 1, [LA] = 1 M in toluene. [b] [LA] : [catalyst] : [BnOH] = 100 : 1 : 1, 403 K. Unless otherwise stated. [c] The theoretical molecular weight calculated from conversion {([LA] : [catalyst] × (% conv.) × 144.13)} or {([LA] : [catalyst] × (% conv./no. eq BnOH × 144.13)) + 108.14}. [d] Determined by GPC analysis calibrated using narrow MW polystyrene standards, in THF and corrected by Mark–Houwink parameter (0.58). [e] Determined by relative integration of PLA methine tetrads in the ^{1}H{^{1}H} NMR spectrum using values predicted according to Bernoullian statistics.[68] [f] $Đ = M_w/M_n$. [g] Determined by integration of the methine region of the ^{1}H NMR spectrum at δ 4.98–5.06 ppm (LA) and δ 5.08–5.22 (PLA).

rates as shown in Fig. 7, as is commonly reported for ROP of lactide proceeding *via* coordination–insertion mechanism.[69,70] The *pseudo* first order rate coefficients (k_{obs}) were obtained from the slopes of these plots. Comparison of the rate constants revealed that **8** and **10** are slightly faster than **9**, which in terms of electronic influence of the ligands substituents implied that complexes containing neutral and electron-withdrawing side chain induced the polymerization more rapidly, reaching nearly complete conversion of the monomer in 1 hour (Table 2, entries 1–3), this observation agrees with previous reports where use of withdrawing groups was proposed to increase the Lewis acidity of the metal and consequently accelerate the polymerization reaction.[71,72] However, greater activity of **8** with unsubstituted glycine ligand over **9** and **10** bearing leucine and threonine ligands (R = alkyl and hydroxyl group, respectively) may be tentatively attributed by decreased steric hindrance in the metal coordination sphere, increasing lability of the metal–carboxylate M–OR bond that subsequently increases the rate of lactide insertion.[50] It is notable that all catalysts show a short induction period. Typically, it was 20 min, and the relative length was independent of the type of catalyst. It is observed that this time period incorporates the time required for the reaction solution to reach the desired temperature from room temperature and subsequently activate the catalyst.

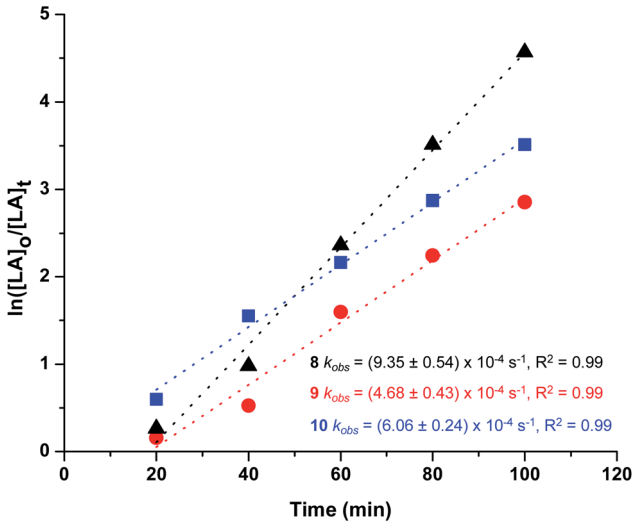

Fig. 7 Pseudo first-order kinetic plot of ln([LA]$_0$/[LA]$_t$) *vs.* time for ROP of *rac*-lactide using complexes **8–10**.

Molecular weights of polymers obtained with **8** (Table 2, entries 1 & 2), as determined experimentally by GPC analysis *i.e.* ($M_{n,obs}$ = 12.39 kg mol^{-1}), were found to be in good agreement with theoretical values ($M_{n,theo}$ = 13.59 kg mol^{-1}) that were calculated assuming the growth of a single polymer chain per active center. This observation is indicative of a well-controlled polymerization. On the contrary, **9** and **10** produced PLA with higher molar mass than expected theoretically. This is most likely due to slow initiation rates relative to propagation rates, usually observed for poor nucleophilicity and sterically hindered initiating group.[9,14] Alternatively, experiments were carried out incorporating one equivalent of BnOH which could undergo fast and reversible reaction exchange between free alcohol and ligands, improving the initiation rate efficiency (Table 2, entries 7 & 8). Interestingly, presence of an exogenous alcohol, was found to both increase polymerization times and impart a significant decrement on catalytic activity. The PLA so obtained showed large and bimodal molecular weight distribution ($Đ$) suggesting that BnOH negatively impacts control of the polymerization. Based on previous literature reports, it is also plausible that two competing mechanisms are active, promoted from two different initiating groups.[73–75] Extended reaction times without incorporation of BnOH resulted in observed broadened polydispersities ($Đ$ = 1.13–1.40, Table 2, entries 4–6), suggesting that chain transfer and intermolecular transesterification reactions may predominate at high conversion >60%, which could be ascribable to the presence of distinct amounts of water in commercial grade *rac*-lactide and the crystal water in the lattice of the complexes accelerating transesterification reaction. Due to the absence of initiator groups or vacant active site in the metal center a mechanistic hypothesis can be proposed to rationalize the formation of PLA as shown in

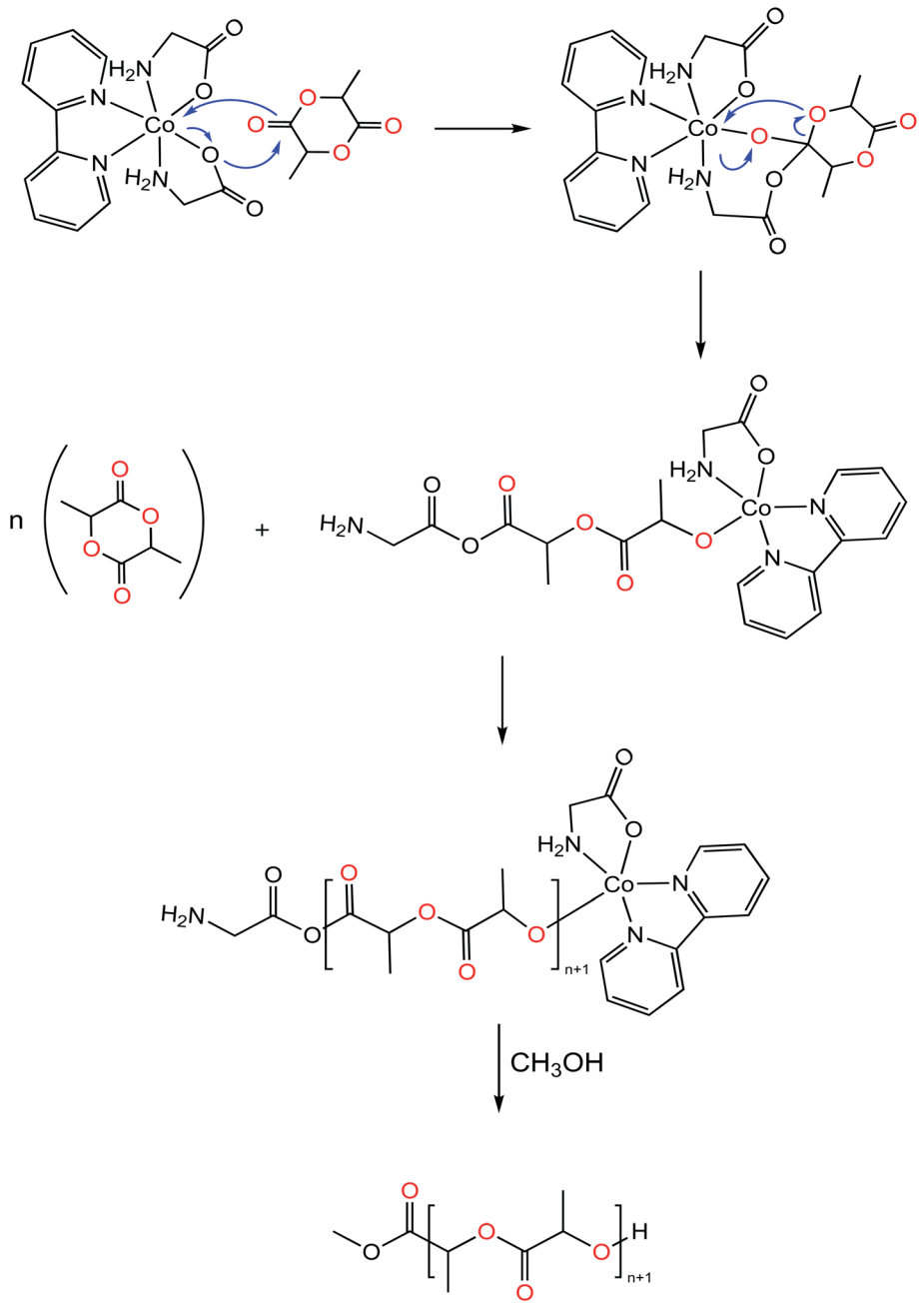

Fig. 8 Proposed pathway for the ROP of LA catalyzed by [Co(aa)$_2$(bipy)].

Fig. 8. The initiator is thermally activated where the Co-carboxylate (Co–O) bond is labilized. Dissociation of the Co–O bond is followed by the coordination of the carbonyl oxygen of the monomer to the metal center, activating thereby it towards attack from the metal–carboxylate bond. Following by monomer insertion into the metal–organic bond formed, through the breakdown of the acyl-oxygen or alkyl–oxygen bond in the cyclic compound. Finally, the polymerization process occurs through concerted process with the consecutive insertion of the monomer molecules in the metal–oxygen bond (in this case Co–O) of the propagating species concurrent with acyl oxygen bond cleavage, termination step occurs with hydrolysis of chain end group in presence of excess of methanol.

To gather further information on the polymer microstructure, tacticity of the polymers was assessed by relative integration of methine resonances in the homonuclear decoupled ^{1}H $\{^1$H$\}$ NMR spectrum (Fig. S36–S38†) for PLA samples, and stereo-sequence (tetrads) probabilities were predicted according to Bernoullian statistical model.[68,76] All catalysts induced at least moderate levels of stereocontrolled microstructure, displaying slightly isotactic bias in resulting polymers (P_i = 0.49–0.65). This observation was correlated to the high reaction temperatures used. As an attempt to enhance stereoselectivity, polymerization reactions were conducted at lower temperatures ≤100 °C which, however, did not result in polymer formation. Co(III) species **1a–3** resulted completely inactive for LA ROP

presumably due to highly stable electronic environment around the metal center, this observation has been reported for other cationic complexes.[77–79]

Conclusion

The synthesis of a series of trimetallic, cationic and neutral cobalt complexes with bipy and amino acids as ligands successfully led to isolation and characterization of several Co(II) and Co(III) complexes. Complex **1** was obtained and characterized in the solid state by X-ray diffraction its structure showed a tetraaquacobaltate chloride(II) co-crystallized in the lattice. Trimetallic species were prepared and oxidized in air in the presence of non-coordinative anion such as PF_6^-. Neutral complexes **8–10** proved to be active as catalysts in the ROP reaction of lactide to form PLA, whereas cationic complexes **1a–3** were inactive. The electronic properties of the complexes can be varied systematically changing the amino acid side chain by a neutral, hydrophilic or hydrophobic and these traits were further assessed in ROP of LA. This system displayed good performance towards lactide polymerization with a moderate isotactic bias. The promising results obtained highlight the potential applicability and future investigation of this catalytic system for mechanistically related polymerizations such as lactone ROP and epoxide/CO_2 ring-opening copolymerization (ROCOP). In summary, the cobalt catalysts are composed of biorelevant ligands, inexpensive metal, and prepared in environmentally friendly solvent to produce a biodegradable polyester. Future work needs to target the amino acid side chain optimization so as to enhance stereoregularity of the polymer.

Experimental section

Materials and methods

Instrumentation. 1D (^{1}H, ^{13}C) and 2D NMR spectra were obtained using Bruker AV 400 MHz spectrometer at room temperature with chemical shifts reported in ppm relative to the residual solvent signal as an internal standard unless otherwise stated. Infrared spectra were obtained as KBr pellets with Nicolet Avatar 360 FT-IR (E.S.P) spectrophotometer in the range of 4000–400 cm^{-1}. UV-visible spectra were recorded on Perkin Elmer, Lambda 25, UV/Vis spectrometer. Mass spectrometric analysis were collected using a Bruker micrOTOF (Bruker autoflex smartbeam) spectrometer as ESI in positive ion electrospray scan. Elemental analysis was performed by Midwest Microlab, IN, USA.

GPC instrumentation. GPC measurements were carried out on two mixed bed PSS SDV linear S gel columns in series, with THF as eluent at a flow rate of 1 mL min^{-1} on a HP1090 II chromatograph with a DAD detector (Hewlett-Packard) at 40 °C. The polyester was dissolved in HPLC grade THF and filtered through a 0.200 μm PTFE porous filter prior analysis. Polymer number-average molecular weight (M_n) and polydispersity index (M_w/M_n; $Đ$) were determined by comparison against narrow polystyrene standards, and the resultant PLA molar mass corrected by Mark–Houwink correction factor of 0.58. The overall tacticity of the PLA was determined from MestRenova v.14.0.0, taking an average of tetrad integrals predicted from Bernoullian statistics.

Solvents and reagents. All experimental manipulations were conducted under N_2 atmosphere using standard Schlenk-line techniques and glassware baked at 120 °C for at least 12 hours prior to use. Solvents and reagents were obtained from commercial sources and used as received unless otherwise stated. MeCN and Et_2O were distilled over sodium wires/benzophenone and stored over activated (3 Å) molecular sieves prior to use. The starting materials were used as supplied from Bachem, Sigma Aldrich, Acros Organics or Fisher Scientific.

Preparation of compounds

Complex 1 $[Co(H_2O)_4\{$*trans*(N)-$[Co(gly)_2(bipy)]\}_2]Cl_2$. To a solution of bipy (0.120 g, 0.770 mmol) in degassed ethanol (20 mL, 70% v/v) was added glyH (0.116 g, 1.540 mmol). The resulting solution was stirred and heated to reflux for 45 min, $CoCl_2$ (0.100 g, 0.770 mmol) was added and the clear solution instantly changed from colourless to pinkish-orange. The reaction mixture was heated for 24 h at 78 °C, under nitrogen. The obtained dark pinkish-orange solution was concentrated to 2 mL under reduced pressure, followed by slow addition of acetone (10 mL), the flask was placed in the freezer. Orange block-shaped crystals formed overnight. Yield: 58% calculated relative to cobalt. FT-IR (KBr disc, ν_{max}/cm^{-1}): 3426(m, br), 3248(m, br), 2980(s, br), 1651(s, C=O), 1607(s, C=O), 1571(w), 1470(mw), 1444(ms), 1393(ms), 929(mw), 769(ms). UV/vis (EtOH, 5×10^{-5} M), λ_{max} (ε, M^{-1} cm^{-1}): 307(19 100), 316(19 860), 491(130).

Complex 1a *trans*(N)-$[Co^{III}(gly)_2(bipy)]Cl\cdot 2H_2O\cdot 0.5CH_3CH_2OH$. To a solution of bipy (0.120 g, 0.770 mmol) in ethanol (20 mL, 70% v/v) was added glyH (0.116 g, 1.540 mmol). The resulting solution was stirred and heated to reflux for 45 min, $CoCl_2$ (0.100 g, 0.770 mmol) was added and the clear solution instantly changed from colourless to pinkish-orange. The reaction mixture was heated for 24 h at 78 °C. The pale pink solution was allowed to warm to room temperature and stir for 1 hour. The obtained dark pinkish-orange solution was concentrated to 2 mL under reduced pressure, followed by addition of diethyl ether (15 mL) to afford a pink solid. Slow vapor diffusion of acetone into concentrate solution of product in aqueous EtOH 70% afforded red needle crystals. Analytical and spectroscopic data were in agreement with previously reported in literature.[48] Yield: (0.23 g, 0.569 mmol, 74%). ^{1}H NMR (D_2O): 8.54 (m, 4H, Ar-**H**, $J = 11.7$, 6.8 Hz), 8.41 (t, 2H, Ar-**H**, $J = 7.9$ Hz), 7.89 (t, 2H, Ar-**H**, $J = 6.7$ Hz), 3.77 (d, 2H, α-**H**, $J = 17.3$ Hz), 3.49 (d, 2H, α-**H**, $J = 17.4$ Hz). (DMSO-d_6): 8.74 (d, 2H, Ar-**H**, $J = 8.1$ Hz), 8.39 (t, 4H, Ar-**H**, $J = 6.4$ Hz), 7.94–7.89 (m, 2H, Ar-**H**), 6.05 (d, 2H, N**H**, $J = 7.1$ Hz), 5.51 (d, 2H, N**H**, $J = 8.7$ Hz), 3.28–3.19 (m, 2H, α-**H**), 3.05 (m, 2H, α-**H**, $J = 16.4$, 8.2 Hz). ^{13}C NMR (DMSO-d_6) 181.69 (**C**OO), 156.87, 150.80, 141.23, 127.16, 123.47, 45.59(α-**C**). FT-IR (KBr disc, ν_{max}/cm^{-1}): 3418(m, br), 3234(m, br), 3086(mw), 1640(s), 1472(w), 1426(w), 1372(ms), 918(mw), 773(mw). Elemental analysis for $C_{14}H_{16}N_4O_4CoCl\cdot 2H_2O\cdot 0.5CH_3CH_2OH$ (465.76 g mol^{-1}): calculated C, 38.68; H,

4.98; N, 12.03%. Found C, 38.52; H, 5.05; N, 12.19%. HRMS (ESI) for $C_{14}H_{16}N_4O_4CoCl$ 363.0498; found 363.0498 ($[M–Cl]^+$).

Complex 2 *trans*(N)-[Co^{III}(leu)$_2$(bipy)]Cl·2H$_2$O. To a solution of bipy (0.120 g, 0.770 mmol) in ethanol (20 mL, 70% v/v) was added leuH (0.202 g, 1.540 mmol). The resulting solution was stirred and heated to reflux for 45 min, $CoCl_2$ (0.100 g, 0.770 mmol) was added and the clear solution instantly changed from colourless to reddish-orange. The reaction mixture was heated for 24 h at 78 °C. The obtained dark red solution was concentrated to 2 mL under reduced pressure, followed by slow addition of Et_2O (10 mL), the flask was placed in the freezer. The product is a pink solid. Crystals were obtained by vapor diffusion of pentane into a concentrate solution of complex in EtOH : DCM : MeCN 1 : 2 : 1 at 3 °C. Dark red crystals were collected. Yield: (0.22 g, 0.430 mmol, 56%). ^{1}H NMR(D_2O): 8.58–8.51 (m, 4H, Ar-**H**), 8.43 (m, 2H, Ar-**H**, J = 7.9, 6.3, 2.8 Hz), 7.90 (m, 2H, Ar-**H**, J = 7.3, 5.9, 2.6, 1.3 Hz), 3.82 (dd, 2H, α-**H**, J = 10.6, 3.5 Hz), 3.59–3.43 (m, 1H, α-**H**), 1.91–1.77 (m, 1H), 1.75–1.57 (m, 4H, C**H**$_2$CH), 1.45 (td, 2H, CH$_2$C**H**, J = 12.1, 10.5, 3.3 Hz), 0.99–0.81 (m, 12H, C**H**$_3$) ppm (DMSO-d_6): 8.80 (d, 2H, Ar-**H**, J = 7.9 Hz), 8.37 (td, 4H, Ar-**H**, J = 14.8, 13.9, 6.8 Hz), 7.89 (dt, 2H, Ar-**H**, J = 13.7, 6.6 Hz), 6.43 (t, 1H, N**H**, J = 9.1 Hz), 6.00 (t, 1H, N**H**, J = 9.3 Hz), 5.54–5.44 (t, 1H, N**H**), 4.97 (t, 1H, N**H**, J = 9.4 Hz), 3.29 (m, 1H, α-**H**, J = 4.8, 4.2 Hz), 3.02 (m, 1H, α-**H**, J = 12.1, 5.7 Hz), 1.94–1.68 (m, 2H, CH$_2$C**H**), 1.63–1.42 (m, 2H, C**H**$_2$CH), 1.30 (m, 2H, C**H**$_2$CH, J = 14.4, 9.7, 3.8 Hz), 0.87 (dd, 6H, C**H**$_3$, J = 11.2, 6.5 Hz), 0.78 (dd, 6H, C**H**$_3$, J = 17.2, 6.5 Hz). ^{13}C NMR (DMSO-d_6) 183.27, 182.74 (2 **C**OO$^-$), 157.48, 157.07, 150.87, 150.78, 141.01, 140.95, 126.87, 126.80, 123.37, 123.19, 54.70, 54.57, 42.41, 23.36, 23.30, 23.25, 20.77, 20.71. FT-IR (KBr disc, ν_{max}/cm^{-1}): 3423(m, br), 3219(m), 3061(m), 2957–2869(ms), 1652(s), 1471(mw), 1451(ms), 1369(ms), 928(w), 771(ms). UV/vis (EtOH, 5×10^{-5} M), λ_{max} (ε, M^{-1} cm^{-1}): 301(7696), 313(8952), 479(109). Elemental analysis for $C_{22}H_{32}N_4O_4CoCl \cdot 2H_2O$ (546.94 g mol^{-1}): calculated C, 48.31; H, 6.63; N 10.24%. Found C, 48.57; H, 6.71; N, 10.10%. HRMS (ESI) for $C_{22}H_{32}N_4O_4CoCl$ 475.1750; Found 475.1750 ($[M–Cl]^+$).

Complex 3 *trans*(N)-[Co^{III}(thr)$_2$(bipy)]Cl·2.5H$_2$O. To a solution of bipy (0.120 g, 0.770 mmol) in ethanol (20 mL, 60% v/v) was added thrH (0.183 g, 1.540 mmol). The resulting solution was stirred and heated to reflux for 45 min, $CoCl_2$ (0.100 g, 0.770 mmol) was added and the clear solution instantly changed from colourless to pink. The reaction mixture was heated for 24 h at 78 °C. The obtained orange solution was concentrated to 2 mL under reduced pressure, followed by slow addition of Et_2O (10 mL), the flask was placed in the freezer. Pale pink solid formed overnight. Yield: (0.21 g, 0.423 mmol, 55%). 1H NMR(D2O): 8.55–8.46 (m, 4H, Ar-**H**), 8.40 (td, 2H, Ar-**H**, J = 7.8, 1.5), 7.86 (ddd, 2H, Ar-**H**, J = 7.5, 5.9, 1.4), 4.38 (m, 2H, C**H**(OH), J = 6.7, 1.6), 3.78 (d, 2H, α-**H**, J = 1.6), 1.21 (d, 6H, C**H**$_3$, J = 6.7) ppm. (DMSO-d_6): 8.70 (d, 2H, Ar-H, J = 8.0 Hz), 8.41–8.30 (m, 4H, Ar-H), 7.81 (t, 2H, Ar-H, J = 6.7 Hz), 6.23 (t, 2H, NH, J = 9.2 Hz), 4.80 (dd, 4H, N**H**, O**H**, J = 13.2, 7.2 Hz), 4.09 (p, 2H, C**H**(OH), J = 6.0, 5.5 Hz), 3.20 (d, 2H, α-**H**, J = 16.5 Hz), 1.10 (d, 6H, C**H**$_3$, J = 6.7 Hz) ppm. ^{13}C NMR (DMSO-d_6): 181.75 (**C**OO), 157.71, 151.17, 140.75, 126.11, 123.01, 66.26, 62.44, 20.25. FT-IR (KBr disc, ν_{max}/cm^{-1}): 3404(m, br), 3085(mw), 2975(w), 1659(s), 1471(w), 1451(m), 1381(m), 995(w), 774(m). UV/vis (EtOH, 5×10^{-5} M), λ_{max} (ε, M^{-1} cm^{-1}): 300(4971), 312(5204), 480(87). Elemental analysis for $C_{18}H_{24}N_4O_6CoCl \cdot 2.5H_2O$ (531.84 g mol^{-1}): calculated C, 40.65; H, 5.50; N, 10.53%. Found C, 40.85; H, 5.47; N, 10.35%. HRMS (ESI) for $C_{18}H_{24}N_4O_6Co$ 451.1022; found 451.1017 ($[M–Cl]^+$).

Trimetallic species **4–6** were all prepared by a similar procedure. The synthesis of **4** is given as an example.

Complex 4 [Co(H$_2$O)$_2$(OAc)$_2${*trans*(N)-[Co(gly)$_2$(bipy)]}$_2$]. An amount of bipy (0.088 g, 0.565 mmol) and glyH (0.085 g, 1.130 mmol) were dissolved in degassed ethanol (20 mL, 70% v/v). The resulting solution was stirred and heated to reflux for 45 min. Next, $Co(CH_3COO)_2$ (0.100 g, 0.565 mmol) was added and the clear solution instantly changed to pinkish-orange. The reaction mixture was heated for 24 h at 78 °C. The obtained pale pink solution was reduced to dryness under reduced pressure. The residue was redissolved in ethanol (2 mL), followed by addition of diethyl ether (15 mL) to afford a pink solid. The pink powder was washed with Et_2O (3 × 10 mL) and dried *in vacuo* overnight. Yield: 63% calculated relative to cobalt. Elemental analysis for $C_{32}H_{42}N_8O_{14}Co_3$ (939.5 g mol^{-1}): calculated C, 40.91; H, 4.51; N 11.93%. Found C, 41.26; H, 4.42; N 11.79%. HRMS (ESI) for $C_{14}H_{16}N_4O_4Co$ 363.0498; found: 363.0505 $[M]^+$.

Complex 4a *trans*(N)-[Co^{III}(gly)$_2$(bipy)][PF$_6$]. The complex **4** (0.100 g, 0.106 mmol) was oxidized by exposure to air and by the addition of 2 equivalents of acetic acid (12.78 μL, 0.213 mmol) in EtOH, the resulting solution was stirred and gently heated up to 50 °C, over 1 hour with reaction progress being monitored using ^{1}H NMR spectroscopy. Once the oxidation was complete, 10 equivalents of (Bu_4N)(PF_6) (0.413 g, 1.07 mmol) was added and stirred for 24 hours. The resulting suspension was filtered, and the filtrate concentrated under reduced pressure and the excess of acetic acid removed by azeotropic distillation with toluene (3 × 20 mL). Red rod crystals suitable for single-crystal X-ray diffraction were grown by slow evaporation of concentrated solution of the product in DCM : EtOH after 2 days. Yield: (0.02 g, 0.043 mmol, 41%). 1H NMR (D2O) 8.59–8.50 (m, 4H, Ar-**H**), 8.44–8.36 (m, 2H, Ar-**H**), 7.89 (t, J = 6.7 Hz, 2H, Ar-**H**), 3.75 (d, 2H, α-**H**, J = 17.4 Hz), 3.48 (d, 2H, α-**H**, J = 17.2 Hz) ppm (DMSO-d_6): 8.75 (d, 2H, Ar-**H**, J = 7.9 Hz), 8.48–8.35 (m, 4H, Ar-**H**), 7.92 (m, 2H, Ar-**H**, J = 7.3, 5.6, 1.3 Hz), 6.08 (t, 2H, N**H**, J = 11.3, 8.6, 4.5 Hz), 5.59 (t, 2H, N**H**, J = 8.1 Hz), 3.33–3.22 (m, 2H, α-**H**), 3.08 (m, 2H, α-**H**, J = 16.5, 8.3 Hz). ^{13}C NMR (DMSO-d_6): 181.68 (**C**OO), 156.86, 150.80, 141.23, 127.16, 123.47, 45.59. FT-IR (KBr disc, ν_{max}/cm^{-1}): 3431(br), 3304(w), 3060(w), 1663(s), 1369(mw), 1317(mw), 845(s), 774(mw), 556(mw). HRMS (ESI) for $C_{14}H_{16}N_4O_4Co$ 363.0498; Found 363.0484 ($[M–PF_6]^+$).

Complex 5 [Co(H$_2$O)$_2$(OAc)$_2${*trans*(N)-[Co(leu)$_2$(bipy)]}$_2$]. The pink powder was washed with Et_2O (3 × 10 mL) and dried *in vacuo* overnight. Yield: 66% calculated relative to cobalt. Elemental analysis for $C_{48}H_{74}N_8O_{14}Co_3$ (1163.96 g mol^{-1}): calculated C, 49.53; H, 6.41; N 9.63%. Found C, 49.29; H, 6.01; N 9.89%. HRMS (ESI) for $C_{22}H_{32}N_4O_4Co$ 475.1750; found 475.1753 $[M]^+$.

Complex 6 [Co(H$_2$O)$_2$(OAc)$_2${*trans*(N)-[Co(thr)$_2$(bipy)]}$_2$]. The pink powder was washed with Et_2O (3 × 10 mL) and dried *in vacuo* overnight. Yield: 78% calculated relative to cobalt.

Elemental analysis for $C_{40}H_{58}N_8O_{18}Co_3$ (1115.74 g mol^{-1}): calculated C, 43.06; H, 5.24; N 10.04%. Found C, 43.86; H, 5.02; N, 10.12%. HRMS (ESI) for $C_{18}H_{24}N_4O_6Co$ 451.1022; found 451.1010 $[M]^+$.

Complex 7 *trans*(N)-[Co^{III}(gly)$_2$(bipy)]NO_3. In an analogous procedure for complex 4 pink powder was obtained. Slow diffusion of acetone into concentrate aqueous ethanol afforded orange block crystals. Yield: (0.08 g, 0.182 mmol, 53%). 1H NMR (D2O): 8.55–8.49 (m, 4H, Ar-**H**), 8.39 (td, 2H, Ar-**H**, J = 7.9, 1.4 Hz), 7.88 (ddd, 2H, Ar-**H**, J = 7.3, 5.7, 1.4 Hz), 3.75 (d, 2H, α-**H**, J = 17.4 Hz), 3.47 (d, J = 17.4 Hz, 2H) ppm (DMSO-d_6): δ = 8.72 (m, 2H, Ar-**H**, J = 8.0, 1.2 Hz), 8.44–8.38 (m, 4H, Ar-**H**), 7.93 (m, 2H, Ar-**H**, J = 7.3, 5.7, 1.3 Hz), 6.09 (t, 2H, N**H**, J = 8.8 Hz), 5.41 (t, 2H, N**H**, J = 8.3 Hz), 3.40–3.37 (m, 2H, α-**H**), 3.09 (m, 2H, α-**H**, J = 16.5, 8.1 Hz) ppm. ^{13}C NMR (DMSO-d_6): δ 181.70 (**C**OO), 156.84, 150.78, 141.20, 127.18, 123.43, 45.46. FT-IR (KBr disc, ν_{max}/cm^{-1}): 3446(br), 3086(mw), 1653(s), 1610(s), 1376(s), 1339(s), 921(w), 776(mw). HRMS (ESI) for $C_{14}H_{16}N_4O_4Co$ 363.0498; found 363.0507 ($[M–NO_3]^+$).

Synthesis of neutral compounds 8–10

Complex 8 *trans*(N)-[Co(gly)$_2$(bipy)]. Under a nitrogen atmosphere, $Co(CH_3COO)_2$ (0.500 g, 2.82 mmol) and glyH (0.424 g, 5.65 mmol) were dissolved in degassed ethanol (100 mL, 70% v/v). The resulting solution was stirred and heated to reflux for 45 min. Next, two equivalents of Et_3N (0.78 mL, 5.65 mmol) were added dropwise to give a pink-white suspension and then bipy (0.441 g, 2.82 mmol) was added. The reaction mixture was heated for 24 h at 78 °C. The solvent was taken to dryness under reduced pressure. The residue was redissolved in ethanol (10 mL) and the purple insoluble solid that formed was filtered off through Celite and silica 60. The filtrate was collected and concentrated to 2 mL, followed by addition of diethyl ether (15 mL) to afford a pink solid. The pink powder was washed with $CHCl_3$ and Et_2O (3 × 20 mL) and dried *in vacuo* overnight. Yield: (0.96 g, 2.660 mmol, 94%) FT-IR (KBr disc, ν_{max}/cm^{-1}): 3418(m, br), 3234(m, br), 3086(mw), 1640(s), 1472(w), 1426(w), 1372(ms), 918(mw), 773(mw). HRMS (ESI) for $C_{14}H_{16}N_4O_4Co$ 363.0498; Found 363.0499 $[M]^+$.

Complex 9 *trans*(N)-[Co(leu)$_2$(bipy)]

*Similar procedure of **8** but employing $CoCl_2$.* The product is a pink solid. Yield: (1.52 g, 3.200 mmol, 83%), FT-IR (KBr disc, ν_{max}/cm^{-1}): 3417(m, br), 3207(m, br), 3080(mw), 2956–2869(mw), 1647(s), 1564(mw), 1471(w), 1450(m), 1388(s), 928(w), 770(m). HRMS (ESI) for $C_{22}H_{32}N_4O_4Co$ 475.1750; found 475.1751 $[M]^+$.

Complex 10 *trans*(N)-[Co(thr)$_2$(bipy)]

*Similar procedure of **8**.* Pink solid. Yield: (1.10 g, 2.430 mmol, 63%), FT-IR (KBr disc, ν_{max}/cm^{-1}): 3396(m, br), 3238(m, br), 3061(w), 2971(mw), 1659(s), 1471 (w), 1421(m), 1373(m), 995(w), 772(m). HRMS (ESI) for $C_{18}H_{24}N_4O_6Co$ 451.1022; found 451.1019 $[M]^+$.

General procedure of polymerization of *rac*-lactide

All the polymerizations were conducted under argon. In a typical experiment a Schlenk flask (10 mL) was charged sequentially with *rac*-lactide (0.357 g, 2.5 mmol), complex (0.025 mmol), and dissolved in toluene (2.5 mL) such that the overall molar ratio was ([LA] : [1] = 100 : 1). The flask was sealed and placed into a hot oil bath set to 403 K. The reaction was stirred for the desired time and aliquots were withdraw at specific time intervals and quenched with $CDCl_3$ to analyze the conversion by relative integration of the methine proton resonances for the polymer and monomer using ^{1}H NMR spectroscopy. Remaining crude polymer mixture was dissolved in $CHCl_3$ (~2 mL) and dropwise added into a solution of acidic cold methanol (~15 mL) to precipitate it. The polymer collected was dried at 30 °C *in vacuo*.

X-ray crystallography. X-ray quality single crystals were obtained by vapor diffusion of either hexane or pentane into a EtOH : DMC : MeCN concentrate solution of the metal complex. The crystals were isolated from the mother liquor, immediately immersed in cryogenic oil and then mounted. The X-ray single crystal data was collected using MoKα (λ = 0.71073 Å) or CuK_α (λ = 1.54178 Å) radiation on a Bruker D8Venture (Photon100 CMOS detector) diffractometer equipped with a Cryostream (Oxford Cryosystems) open-flow nitrogen cryostats at the temperature 150(2) K. The unit cell determination, data collection, data reduction, structure solution/refinement and empirical absorption correction (SADABS) were carried out using Apex-III (Bruker AXS: Madison, WI, 2015). The structure was solved by direct method and refined by full-matrix least squares in F^2 for all data using SHELXTL[80] and Olex2 (ref. 81) software. All non-disordered non-hydrogen atoms were refined anisotropically except for the carbon atoms in **2** which was refined using FVAR instructions and the hydrogen atoms were placed in the calculated positions and refined in riding model. Complex **2** and **7** were refined as an inversion twin we could not model the disordered solvent in **2**, **4a** and **9a**, which was located in the Fourier map, and the contribution of the electron densities from the disordered solvent molecules was excluded from the refinement using PLATON/SQUEEZE.[73] This resulted in the removal of the solvent molecules in **2** corresponding to 93 electron per unit cell, which can be assigned as four acetonitrile molecules per unit cell. The disordered solvent molecule in **4a** could be assigned as five ethanol molecules per unit cell (124 electron per unit cell) and the 360 electron per unit cell in **9a** can be assigned to two dichloromethane molecules. Crystallographic data for the structures have been deposited to Cambridge Crystallographic Data Centre as supplementary publication (CCDC no. 2060291–2060294 and 2062819–2062821†).[82]

Abbreviations

Bipy	2,2-Bipyridine
BnOH	Benzyl alcohol
Đ	Number-average molecular weight distribution
DCM	Dichloromethane
EtOH	Ethanol
gly	Deprotonated glycine
glyH	Protonated glycine

HRMS	High-resolution mass spectrometry
Leu	Deprotonated leucine
LeuH	Protonated leucine
MeCN	Acetonitrile
M_n	Number-average molecular weight
OAc	Acetate
rac-LA	Lactide dimer(monomer)
ROP	Ring opening polymerization
thr	Deprotonated threonine
thrH	Protonated threonine

Conflicts of interest

The authors have no conflicts to declare.

Acknowledgements

Funding from the Icelandic Centre of Research (Rannis) grant no. 152323 is gratefully acknowledged. We thank Rannís Iceland for infrastructure grant for the single crystal X-ray diffractometer (150998-0031). Dr Sigridur Jonsdottir is thanked for assistance with the collection of mass spectrometry data. Dr Esteban Mejia and MSc. Lea Grefe at the Leibniz Institute for Catalysis, (LIKAT), Germany, are acknowledged for their help with GPC and homonuclear decoupling NMR data collection.

References

1 M. He, Y. Cheng, Y. Liang, M. Xia, X. Leng, Y. Wang, Z. Wei, W. Zhang and Y. Li, *Polym. J.*, 2020, **52**, 567–574.
2 M. Fuchs, S. Schmitz, P. M. Schäfer, T. Secker, A. Metz, A. N. Ksiazkiewicz, A. Pich, P. Kögerler, K. Y. Monakhov and S. Herres-Pawlis, *Eur. Polym. J.*, 2020, **122**, 109302.
3 V. M. Padilla-Gainza, H. Rodríguez-Tobías, G. Morales, E. Saucedo-Salazar, K. Lozano, V. Montaño-Machado and D. Mantovani, *J. Appl. Polym. Sci.*, 2021, **138**, 1–13.
4 F. Emami, S. J. Mostafavi Yazdi and D. H. Na, *J. Pharm. Invest.*, 2019, **49**, 427–442.
5 M. N. Abu Hajleh, A. AL-Samydai and E. A. S. Al-Dujaili, *J. Cosmet., Dermatol. Sci. Appl.*, 2020, **19**, 2805–2811.
6 M. Shaver and A. Buchard, *Eur. Polym. J.*, 2020, **129**, 109600.
7 N. Nomura, R. Ishii, Y. Yamamoto and T. Kondo, *Chem.–Eur. J.*, 2007, **13**, 4433–4451.
8 P. Marin, M. J. L. Tschan, F. Isnard, C. Robert, P. Haquette, X. Trivelli, L. Chamoreau, V. Guérineau, I. del Rosal, L. Maron, V. Venditto and C. M. Thomas, *Angew. Chem., Int. Ed.*, 2019, **58**, 12585–12589.
9 N. Yuntawattana, T. M. McGuire, C. B. Durr, A. Buchard and C. K. Williams, *Catal. Sci. Technol.*, 2020, **10**, 7226–7239.
10 D. Myers, A. J. P. White, C. M. Forsyth, M. Bown and C. K. Williams, *Angew. Chem., Int. Ed.*, 2017, **56**, 5277–5282.
11 P. M. Schäfer and S. Herres-Pawlis, *ChemPlusChem*, 2020, **85**, 1044–1052.
12 Y. Gong and H. Ma, *Chem. Commun.*, 2019, **55**, 10112–10115.
13 W. Gruszka, A. Lykkeberg, G. S. Nichol, M. P. Shaver, A. Buchard and J. A. Garden, *Chem. Sci.*, 2020, **11**, 11785–11790.
14 C. Bakewell, T.-P.-A. Cao, N. Long, X. F. Le Goff, A. Auffrant and C. K. Williams, *J. Am. Chem. Soc.*, 2012, **134**, 20577–20580.
15 M. R. Kember, A. J. P. White and C. K. Williams, *Macromolecules*, 2010, **43**, 2291–2298.
16 M. R. Kember, F. Jutz, A. Buchard, A. J. P. White and C. K. Williams, *Chem. Sci.*, 2012, **3**, 1245.
17 Y. Hiranoi and K. Nakano, *Beilstein J. Org. Chem.*, 2018, **14**, 2779–2788.
18 D. Dolui, S. Das, J. Bharti, S. Kumar, P. Kumar and A. Dutta, *Cell Rep. Phys. Sci.*, 2020, **1**, 100007.
19 H. Ullah, B. Mousavi, H. A. Younus, Z. A. K. Khattak, S. Chaemchuen, S. Suleman and F. Verpoort, *Commun. Chem.*, 2019, **2**, 1–9.
20 K. Ambrose, K. N. Robertson and C. M. Kozak, *Dalton Trans.*, 2019, **48**, 6248–6260.
21 T. A. Zevaco and A. W. Kleij, in *Non-Noble Metal Catalysis*, Wiley-VCH Verlag GmbH & Co. KGaA, Weinheim, Germany, 2018, vol. 19, pp. 529–547.
22 A. C. Deacy, E. Moreby, A. Phanopoulos and C. K. Williams, *J. Am. Chem. Soc.*, 2020, **142**, 19150–19160.
23 J. Zhang, B. Wang, L. Wang, J. Sun, Y. Zhang, Z. Cao and Z. Wu, *Appl. Organomet. Chem.*, 2018, **32**, 1–12.
24 P. Marin, M. J. L. Tschan, P. Haquette, T. Roisnel, I. del Rosal, L. Maron and C. M. Thomas, *Eur. Polym. J.*, 2019, **120**, 109208.
25 L. E. Breyfogle, C. K. Williams, V. G. Young, M. A. Hillmyer and W. B. Tolman, *Dalton Trans.*, 2005, **6**, 928–936.
26 C. Thomas and J. A. Gladysz, *ACS Catal.*, 2014, **4**, 1134–1138.
27 M. J. L. Tschan, J. Guo, S. K. Raman, E. Brulé, T. Roisnel, M. N. Rager, R. Legay, G. Durieux, B. Rigaud and C. M. Thomas, *Dalton Trans.*, 2014, **43**, 4550–4564.
28 A. K. Renfrew, E. S. O'Neill, T. W. Hambley and E. J. New, *Coord. Chem. Rev.*, 2018, **375**, 221–233.
29 N. P. Boralugodage, R. J. Arachchige, A. Dutta, G. W. Buchko and W. J. Shaw, *Catal. Sci. Technol.*, 2017, **7**, 1108–1121.
30 M. Hapke and G. Hilt, *Cobalt Catal. Org. Synth.*, 2020, 1–23.
31 H. Shimakoshi and Y. Hisaeda, in *Advances in Bioorganometallic Chemistry*, Elsevier Inc., Fukuoka, Japan, 2019, pp. 379–398.
32 D. J. Darensbourg and O. Karroonnirun, *Inorg. Chem.*, 2010, **49**, 2360–2371.
33 S. L. Anderson and K. C. Stylianou, *Coord. Chem. Rev.*, 2017, **349**, 102–128.
34 X. L. Wang, H. Chao, X. L. Hong, Y. J. Liu and L. N. Ji, *Transition Met. Chem.*, 2005, **30**, 305–311.
35 T. Kondori, O. Shahraki, N. Akbarzadeh-T and Z. Arameshi-Boroujeni, *J. Biomol. Struct. Dyn.*, 2021, **39**, 595–609.
36 J. Börner, U. Flörke, A. Döring, D. Kuckling, M. D. Jones and S. Herres-Pawlis, *Sustainability*, 2009, **1**, 1226–1239.
37 A. Sanchez-Sanchez, I. Rivilla, M. Agirre, A. Basterretxea, A. Etxeberria, A. Veloso, H. Sardon, D. Mecerreyes and F. P. Cossío, *J. Am. Chem. Soc.*, 2017, **139**, 4805–4814.

38 Y. Yan, E. J. Carrington, R. Pétuya, G. F. S. Whitehead, A. Verma, R. K. Hylton, C. C. Tang, N. G. Berry, G. R. Darling, M. S. Dyer, D. Antypov, A. P. Katsoulidis and M. J. Rosseinsky, *J. Am. Chem. Soc.*, 2020, **142**, 14903–14913.
39 Y. Shi, S. Hou, X. Qiu and B. Zhao, *Top. Curr. Chem.*, 2020, **378**, 11.
40 S. L. Anderson and K. C. Stylianou, *Coord. Chem. Rev.*, 2017, **349**, 102–128.
41 I. Burneo, K. C. Stylianou, I. Imaz and D. Maspoch, *Chem. Commun.*, 2014, **50**, 13829–13832.
42 W. J. Shaw, *Catal. Rev. - Sci. Eng.*, 2012, **54**, 489–550.
43 H. Sigel and R. B. Martin, *Chem. Rev.*, 1982, **82**, 385–426.
44 R. Griesser and H. Sigel, *Inorg. Chem.*, 1971, **10**, 2229–2232.
45 L. Rulíšek and Z. Havlas, *J. Am. Chem. Soc.*, 2000, **122**, 10428–10439.
46 B. E. Douglas and T. Yasui, *Inorg. Chem.*, 1971, **10**, 97–102.
47 T. Yasui, *Bull. Chem. Soc. Jpn.*, 1975, **48**, 454–457.
48 R. M. Hartshorn and S. G. Telfer, *J. Chem. Soc., Dalton Trans.*, 1999, 3217–3224.
49 A. Wojciechowska, A. Gagor, A. Duczmal, M. Staszak and Z. Ozaroswski, *Inorg. Chem.*, 2013, **52**, 4360–4371.
50 L. M. Alcazar-Roman, B. J. O'Keefe, M. A. Hillmyer and W. B. Tolman, *Dalton Trans.*, 2003, **15**, 3082–3087.
51 A. Dutta, D. L. Du Bois, J. A. S. Roberts and W. J. Shaw, *Proc. Natl. Acad. Sci. U. S. A.*, 2014, **111**, 16286–16291.
52 K. Arun Kumar, M. Amuthaselvi and A. Dayalan, *Acta Crystallogr., Sect. E: Struct. Rep. Online*, 2011, **E67**(4), m468.
53 A. E. Martell and R. D. Hancock, *Metal Complexes in Aqueous Solutions*, Springer US, Boston, MA, 1996.
54 J. Na'aliya and H. Aliyu, *Bayero J. Pure Appl. Sci.*, 2011, **3**, 52–55.
55 E. Cardozo, C. RR, F. Bellandi, J. Avendaño, C. Araque and J. Vielma, *Rev. Politec.*, 2015, **36**, 1–5.
56 B. Ye, X. Chen and T. Zeng, *Polyhedron*, 1994, **13**, 2185–2191.
57 U. K. Das, J. Bobak, C. Fowler, S. E. Hann, C. F. Petten, L. N. Dawe, A. Decken, F. M. Kerton and C. M. Kozak, *Dalton Trans.*, 2010, **39**, 5462.
58 B. H. Ye, T. X. Zeng, P. Han and L. N. Ji, *Transition Met. Chem.*, 1993, **18**, 515–517.
59 T. Balakrishnan, P. Revathi, A. Krishnaveni, J. Thirupathy and K. Ramamurthi, *J. Mater. Sci.: Mater. Electron.*, 2018, **29**, 16971–16982.
60 L. Gobinathan and K. Boopathy, *J. Adv. Chem.*, 2016, **12**, 5446–5453.
61 M. M. Alam, S. M. S. Islam, S. M. M. Rahman and M. M. Rahman, *J. Sci. Res.*, 2009, **2**, 91–98.
62 A. Tatehata, *Inorg. Chem.*, 1982, **21**, 2496–2499.
63 D. F. Evans, *J. Chem. Soc.*, 1959, 2003–2005.
64 A. C. Rizzi, C. D. Brondino, R. Calvo, R. Baggio, M. T. Garland and R. E. Rapp, *Inorg. Chem.*, 2003, **42**, 4409–4416.
65 D. Das, A. Banaspati, N. Das, B. Bora, M. K. Raza and T. K. Goswami, *Dalton Trans.*, 2019, **48**, 12933–12942.
66 V. Mishra, F. Lloret and R. Mukherjee, *Inorg. Chim. Acta*, 2006, **359**, 4053–4062.
67 F.-L. Yin, R. Xie, J. Hao, Y.-F. Wang and J.-J. Yang, *Inorg. Chem. Commun.*, 2013, **30**, 97–104.
68 M. Cheng, A. B. Attygalle, E. B. Lobkovsky and G. W. Coates, *J. Am. Chem. Soc.*, 1999, **121**, 11583–11584.
69 M. J. Stanford and A. P. Dove, *Chem. Soc. Rev.*, 2010, **39**, 486–494.
70 D. Li, B. Gao and Q. Duan, *New J. Chem.*, 2019, **43**, 6943–6950.
71 S. L. Hancock, M. F. Mahon and M. D. Jones, *Dalton Trans.*, 2013, **42**, 9279–9285.
72 P. M. Schäfer, K. Dankhoff, M. Rothemund, A. N. Ksiazkiewicz, A. Pich, R. Schobert, B. Weber and S. Herres-Pawlis, *ChemistryOpen*, 2019, **8**, 1020–1026.
73 A. J. Gaston, G. Navickaite, G. S. Nichol, M. P. Shaver and J. A. Garden, *Eur. Polym. J.*, 2019, **119**, 507–513.
74 A. Rae, A. J. Gaston, Z. Greindl and J. A. Garden, *Eur. Polym. J.*, 2020, **138**, 109917.
75 C. Robert, T. E. Schmid, V. Richard, P. Haquette, S. K. Raman, M. N. Rager, R. M. Gauvin, Y. Morin, X. Trivelli, V. Guérineau, I. Del Rosal, L. Maron and C. M. Thomas, *J. Am. Chem. Soc.*, 2017, **139**, 6217–6225.
76 D. C. Aluthge, J. M. Ahn and P. Mehrkhodavandi, *Chem. Sci.*, 2015, **6**, 5284–5292.
77 A. B. Biernesser, B. Li and J. A. Byers, *J. Am. Chem. Soc.*, 2013, **135**, 16553–16560.
78 J. A. Byers, A. B. Biernesser, K. R. Delle Chiaie, A. Kaur and J. A. Kehl, *Adv. Polym. Sci.*, 2017, **279**, 67–118.
79 M. Qi, Q. Dong, D. Wang and J. A. Byers, *J. Am. Chem. Soc.*, 2018, **140**, 5686–5690.
80 G. M. Sheldrick, *Acta Crystallogr., Sect. A: Found. Crystallogr.*, 2015, **71**, 3–8.
81 O. V. Dolomanov, L. J. Bourhis, R. J. Gildea, J. A. K. Howard and H. Puschmann, *J. Appl. Crystallogr.*, 2009, **42**, 339–341.
82 G. M. Sheldrick, *Acta Crystallogr., Sect. C: Struct. Chem.*, 2015, **71**, 3–8.